



## Intermediate-Temperature NO<sub>x</sub> Sensor Based on an In<sup>3+</sup>-Doped SnP<sub>2</sub>O<sub>7</sub> Proton Conductor

Masahiro Nagao,<sup>a,\*</sup> Yousuke Namekata,<sup>a</sup> Takashi Hibino,<sup>a,\*\*,z</sup> Mitsuru Sano,<sup>a</sup> and Atsuko Tomita<sup>b</sup>

<sup>a</sup>Graduate School of Environmental Studies, Nagoya University, Nagoya 464-8601, Japan

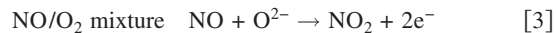
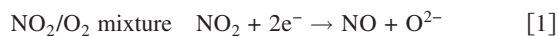
<sup>b</sup>Materials Research Institute for Sustainable Development, National Institute of Advanced Industrial Science and Technology, Moriyama-ku, Nagoya 463-8560, Japan

A potentiometric NO<sub>x</sub> sensor using a proton-conducting Sn<sub>0.9</sub>In<sub>0.1</sub>P<sub>2</sub>O<sub>7</sub> electrolyte with a PtRh/C working electrode was fabricated to study sensing properties for NO and NO<sub>2</sub> at intermediate temperatures. The sensor showed electromotive force (emf) responses to changes in NO and NO<sub>2</sub> concentrations. Interestingly, the emf values for both NO and NO<sub>2</sub> increased in the positive direction with increasing gas concentration. The sensing mechanism was shown to be based on a mixed potential at the working electrode through measurements of the polarization curves of NO or NO<sub>2</sub> and water vapor.

© 2006 The Electrochemical Society. [DOI: 10.1149/1.2193073] All rights reserved.

Manuscript submitted December 19, 2005; revised manuscript received February 22, 2006. Available electronically April 7, 2006.

There has been considerable recent demand for the direct detection of NO<sub>x</sub> in combustion exhausts from automobiles to establish control systems for the reduction of the NO<sub>x</sub> emissions. At present, conventional NO<sub>x</sub> sensors signal a limiting current associated with electrochemical NO decomposition,<sup>1,2</sup> which requires using an expensive two-chamber cell structure connected in series. In addition, the limiting current of a few microamperes or lower is not sufficiently high to assure a high S/N ratio. Thus, the automobile industry needs alternate inexpensive and innovative NO<sub>x</sub> sensors. Potentiometric gas sensors inherently have low manufacturing costs because of their simple cell structure. Moreover, the voltage signal can be more easily amplified when compared to the current signal. Mixed-potential-type gas sensors are promising sensing devices for monitoring low concentrations of pollutants, such as H<sub>2</sub>,<sup>3-5</sup> CO,<sup>6,7</sup> H<sub>2</sub>S,<sup>8</sup> and hydrocarbons,<sup>9-14</sup> in exhausts. Miura et al. were the first to report this type of NO<sub>x</sub> sensor using yttria-stabilized zirconia (YSZ) as the electrolyte.<sup>15</sup> According to the sensing mechanism proposed by them,<sup>16,17</sup> the mixed potential is obtained by coupling the following electrochemical reactions at the working electrode

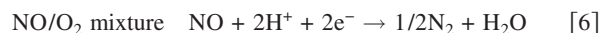
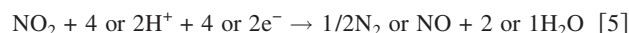


As a result, the potential of the working electrode is shifted toward the positive direction with increasing NO<sub>2</sub> concentration and toward the negative direction with increasing NO concentration. Indeed, some research groups have reported opposite signals for the potential based on NO<sub>2</sub> and NO.<sup>15-19</sup> However, it should be noted that such signals complicate the interpretation of a mixed potential for NO/NO<sub>2</sub> mixtures in actual applications.

We recently reported that an anhydrous proton conductor, 10 mol % In<sup>3+</sup>-doped SnP<sub>2</sub>O<sub>7</sub> (Sn<sub>0.9</sub>In<sub>0.1</sub>P<sub>2</sub>O<sub>7</sub>), shows high proton conductivities >10<sup>-1</sup> S cm<sup>-1</sup> between 150 and 350°C.<sup>20</sup> Attempts to apply this material as the electrolyte in some electrochemical devices were also described. A H<sub>2</sub>-air fuel cell using 0.35 mm thick Sn<sub>0.9</sub>In<sub>0.1</sub>P<sub>2</sub>O<sub>7</sub> electrolyte yielded a power density of 264 mW cm<sup>-2</sup> at 250°C.<sup>21</sup> In addition, an electrochemical reactor using the Sn<sub>0.9</sub>In<sub>0.1</sub>P<sub>2</sub>O<sub>7</sub> electrolyte with a PtBa/C cathode reduced NO<sub>x</sub> to N<sub>2</sub> with a current efficiency of 5.81% at 250°C in oxidizing atmospheres.<sup>22</sup> This material also has the potential to be used for

NO<sub>x</sub> sensor applications because the following electrochemical reactions can be expected to occur at the working electrode

NO<sub>2</sub>/O<sub>2</sub> mixture



These reactions suggest that both NO and NO<sub>2</sub> undergo cathodic reaction at the working electrode, thus providing a common shift of the mixed potential towards the positive direction.

The purpose of this study was to demonstrate the above suggestion by fabricating sensor elements using the Sn<sub>0.9</sub>In<sub>0.1</sub>P<sub>2</sub>O<sub>7</sub> electrolyte. Pt/C and PtRh/C electrodes were chosen as the working electrodes due to high catalytic activities of Pt and Rh metals for the reduction of NO<sub>x</sub>.<sup>23</sup> The sensing properties of these sensors were tested at temperatures of 200°C or higher because Pt metal shows high CO tolerance under such conditions.<sup>24</sup> The dependences of sensing properties on the concentrations of other gases, including water vapor, O<sub>2</sub>, and CO<sub>2</sub>, were also evaluated to clarify the sensing mechanism of the present sensor.

### Experimental

Figure 1 shows a sensor element used for NO<sub>x</sub> sensing tests in this study. Sn<sub>0.9</sub>In<sub>0.1</sub>P<sub>2</sub>O<sub>7</sub> was prepared in the same manner as previously reported.<sup>20,22</sup> The corresponding oxides (SnO<sub>2</sub> and In<sub>2</sub>O<sub>3</sub>) were mixed with 85% H<sub>3</sub>PO<sub>4</sub> and ion-exchanged water and then held with stirring at 300°C until a high viscosity paste was formed. The paste was calcined in an alumina pot at 650°C for 2.5 h and then ground in a mortar with a pestle. Finally, the compound powders were pressed into pellets (12 mm diam, 1.0–1.2 mm thick) under a pressure of 2 × 10<sup>3</sup> kg cm<sup>-2</sup>.

Pt/C (10 wt % Pt/C) and PtRh/C (10 wt % PtRh/C, Pt:Rh = 4:1) electrodes were purchased from E-TEK Inc. A Pt reference electrode was attached on the side face of the electrolyte pellet. The working electrode was supplied with a mixture of 0–1000 ppm NO or 0–1000 ppm NO<sub>2</sub> and 0.6–11.1% water vapor, 2–8% O<sub>2</sub>, and 0–10% CO<sub>2</sub> in Ar at a flow rate of 100 mL min<sup>-1</sup>. The counter and reference electrodes were statically exposed to atmospheric air. The difference in potential (electromotive force, emf) between the working and counter electrodes was measured as a sensing signal with a digital electrometer (Hokuto Denko, HE-104). The polarization curves were measured in 200, 600, and 1000 ppm NO, or 200, 400, and 600 ppm NO<sub>2</sub> diluted with Ar and in 2.7% water vapor diluted with Ar by controlling the potential of the working electrode vs the reference electrode with a potentiostat (Hokuto Denko, HA-501).

\* Electrochemical Society Student Member.

\*\* Electrochemical Society Active Member.

<sup>z</sup> E-mail: hibino@urban.env.nagoya-u.ac.jp

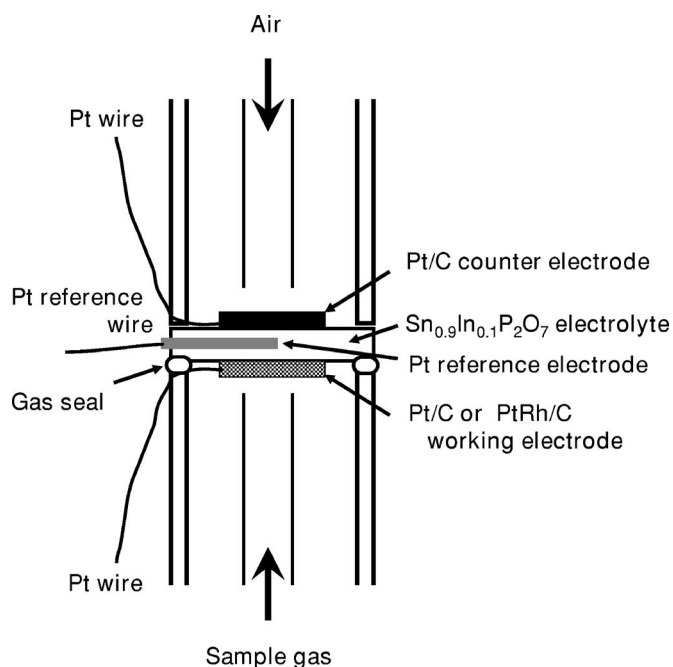


Figure 1. Schematic illustration of the electrochemical cell.

### Results and Discussion

The response transients of the sensors with the Pt/C and PtRh/C working electrodes to NO and NO<sub>2</sub> were first measured at a temperature of 250°C. Figure 2 shows the results when mixtures of 200, 400, and 600 ppm NO or 200, 400, and 600 ppm NO<sub>2</sub> and 2.7% water vapor and 4% O<sub>2</sub> were fed into the working electrode. It was found that both the Pt/C and PtRh/C working electrodes yielded emf responses, depending on the NO and NO<sub>2</sub> concentrations. Characteristically, the extent of the emf response (defined as sensitivity) observed for these working electrodes was larger for NO<sub>2</sub> than for NO under the same conditions. Similar differences in the sensitivity between NO and NO<sub>2</sub> were reported for the YSZ-based NOx sensors.<sup>15-19</sup> It can also be seen from Fig. 2 that the PtRh/C working electrode showed higher sensitivities for NO and NO<sub>2</sub> than the Pt/C working electrode. Nanba et al. have indicated that the catalytic activity of a Pt catalyst for the selective reduction of NOx with H<sub>2</sub> was enhanced by the addition of a small amount of Rh.<sup>25</sup> It seems that Reactions 5 and 6 are similarly promoted for the PtRh/C working electrode, yielding higher sensitivities with the PtRh/C working electrode. However, it cannot be neglected that Reaction 7 is more

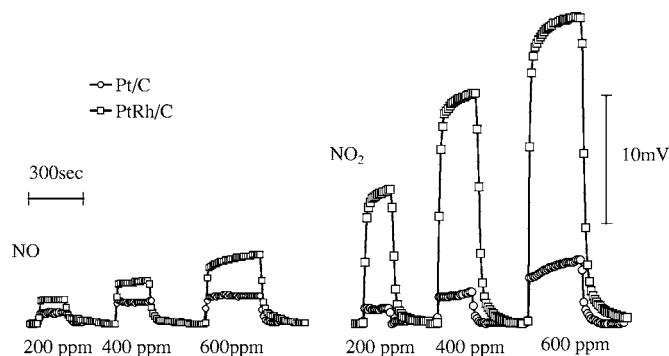


Figure 2. EMF responses of sensors with Pt/C and PtRh/C working electrodes to changes in NO and NO<sub>2</sub> concentrations at 250°C. The water-vapor and O<sub>2</sub> concentrations were maintained at constant values of 2.7 and 4%, respectively.

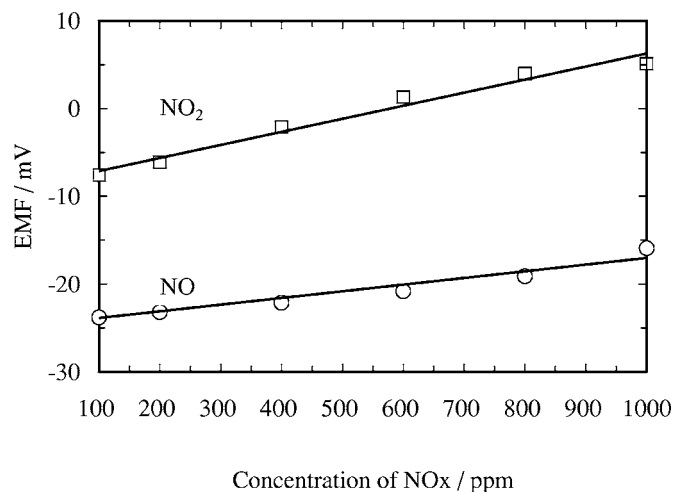


Figure 3. Dependences of emf values for NO and NO<sub>2</sub> on gas concentration at 250°C. The water-vapor and O<sub>2</sub> concentrations were maintained at constant values of 2.7 and 4%, respectively.

inhibited at the PtRh/C electrode as compared to the Pt/C electrode. This will also provide higher sensitivities for the PtRh/C working electrode. Another important result in Fig. 2 is that the direction of the emf response was positive for both NO and NO<sub>2</sub>, indicating a distinguishable characteristic from the results reported for the YSZ-based NOx sensors.<sup>15-19</sup> Preliminary experiments showed that about 9% of the supplied NO was converted into NO<sub>2</sub> through the heterogeneous oxidation on the PtRh/C working electrode, suggesting that the contribution of the converted NO<sub>2</sub> to the emf response for NO is small. This also means the validity of Reactions 5-7. Based on the above results, the sensor with the PtRh/C working electrode was employed in subsequent experiments.

Plots of the emf values as a function of the NO or NO<sub>2</sub> concentration at 250°C are shown in Fig. 3, wherein the concentrations of water vapor and O<sub>2</sub> were maintained at constant values of 2.7 and 4%, respectively. At a NO or NO<sub>2</sub> concentration of 0 ppm, the sensor showed emf values of about -25 mV, which is almost in agreement with the theoretical value (Nernst potential) based on a steam concentration cell<sup>26</sup>

$$E = (RT/2F) \ln \left\{ \frac{P_{H_2O(WE)}}{P_{H_2O(CE)}} \left[ \frac{P_{O_2(CE)}}{P_{O_2(WE)}} \right]^{1/2} \right\} \quad [8]$$

where the forward and reverse reactions of Reaction 7 take place at the working and counter electrodes, respectively. As can be seen in Fig. 3, the emf value increased in the positive direction with increasing NO or NO<sub>2</sub> concentration. There was an approximately linear relationship between the emf value and the NO or NO<sub>2</sub> concentration. These results suggest the possibility that the present sensor could be used to determine the total NOx (NO and NO<sub>2</sub>) concentration, although the low sensitivity to NO must be improved.

If the sensing mechanism of the present sensor is based on the mixed potential resulting from Reactions 5-7, it can be assumed that Reaction 5 or 6 and Reaction 7 simultaneously proceed at the working electrode. These reaction rates are equal to each other due to the formation of a local cell at the working electrode, resulting in the appearance of a mixed potential. To clarify this mechanism, we measured the cathodic polarization curves of 200, 600, and 1000 ppm NO or 200, 400, and 600 ppm NO<sub>2</sub> under dry conditions, and the anodic polarization curve of 2.7% water vapor in the absence of NO and NO<sub>2</sub> at 250°C. The results are summarized in Fig. 4, wherein the direction of the cathodic current is reversed. The cathodic polarization curves for both NO and NO<sub>2</sub> were shifted toward the positive direction with increasing gas concentration. This tendency was especially remarkable for NO<sub>2</sub>. As a result, the intersection points of the anodic and cathodic polarization curves,

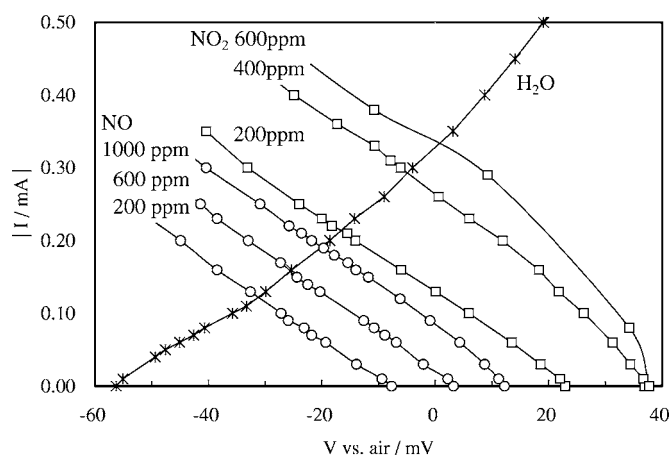
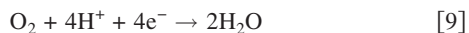


**Figure 4.** Cathodic polarization curves for 200–1000 ppm NO and 200–600 ppm NO<sub>2</sub>, and anodic polarization curve for 2.7% water vapor at 250°C. The direction of the cathodic current is reversed.

which correspond to the mixed potentials, were at  $-31$ ,  $-25$ , and  $-19$  mV for 200, 600, and 1000 ppm NO, respectively, and  $-16$ ,  $-4$ , and  $0$  mV for 200, 400, and 600 ppm NO<sub>2</sub>, respectively. Although these mixed potentials qualitatively explain the results shown in Fig. 2 and 3, they are somewhat less positive than the observed emf values of  $-23$ ,  $-20$ , and  $-15$  mV for 200, 600, and 1000 ppm NO, respectively, and  $-6$ ,  $-2$ ,  $1$  mV for 200, 400, and 600 ppm NO<sub>2</sub>, respectively. One possible explanation for this discrepancy is that the following cathodic reaction also contributes to the emf value when NO<sub>x</sub> coexists with O<sub>2</sub>



Because this reaction participates in the cathodic reaction together with Reactions 5 and 6, the emf values measured in the presence of O<sub>2</sub> can be considered to be more positive than the mixed potential measured in the absence of O<sub>2</sub>.

To better understand the above mechanism, the dependences of the sensitivities to NO and NO<sub>2</sub> on water vapor, O<sub>2</sub>, and CO<sub>2</sub> concentrations were measured at 250°C. As shown in Fig. 5, the sensitivities to NO and NO<sub>2</sub> increased with decreasing water-vapor concentration. This can be explained by an increase in the polarization resistance of Reaction 7 with decreasing water-vapor concentration. Namely, as the polarization resistance of Reaction 7 increases, the

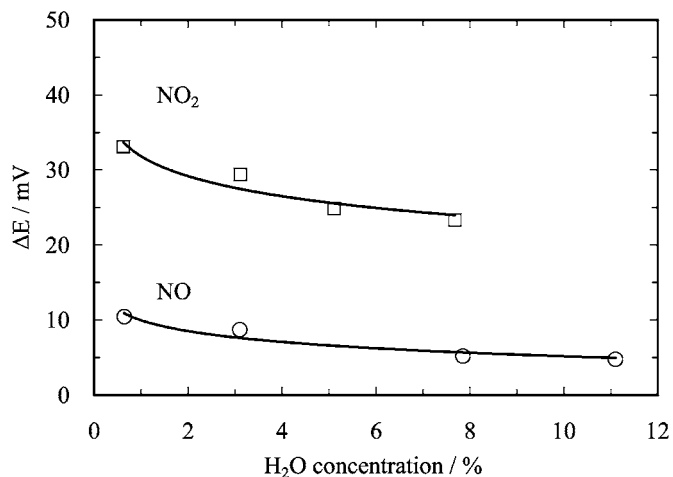


**Figure 5.** Dependences of sensitivities to 1000 ppm NO and 1000 ppm NO<sub>2</sub> on water-vapor concentration at 250°C. The O<sub>2</sub> concentration was maintained at a constant value of 4%.

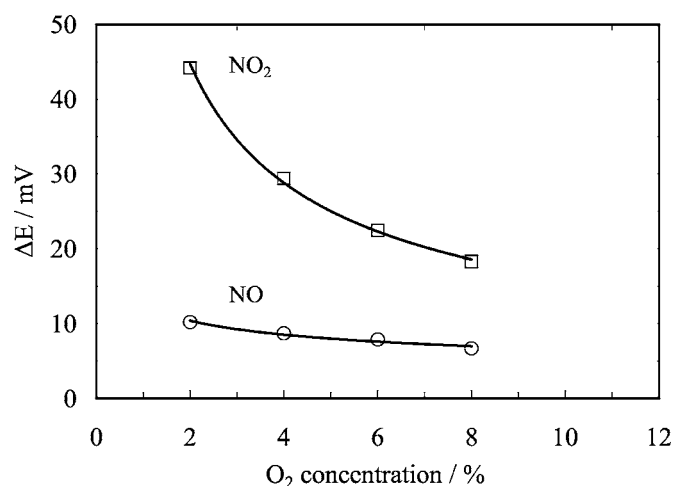


**Figure 6.** Dependences of sensitivities to 1000 ppm NO and 1000 ppm NO<sub>2</sub> on O<sub>2</sub> concentration at 250°C. The water-vapor concentration was maintained at a constant value of 2.7%.

intersection of the anodic and cathodic polarization curves becomes more positive. This dependence is similar to the dependence of the sensitivities to NO and NO<sub>2</sub> in the YSZ-based NO<sub>x</sub> sensors on the O<sub>2</sub> concentration.<sup>15-19</sup> As shown in Fig. 6, the sensitivities to NO and NO<sub>2</sub> also increased with decreasing O<sub>2</sub> concentration. As described earlier, Reactions 5 and 6 compete with Reaction 9 at the working electrode. Because the reaction kinetics of these reactions naturally depend on their gas concentrations, Reaction 5 or 6 contributes to the mixed potential more than Reaction 9 at low O<sub>2</sub> concentrations. On the other hand, in contrast to the results shown in Fig. 5 and 6, the NO and NO<sub>2</sub> sensitivities were seen to be independent of the CO<sub>2</sub> concentration in Fig. 7. This is strong evidence that CO<sub>2</sub> functions as an inert gas for the mixed potential at the working electrode. Similarly, a small amount of CO and hydrocarbons were found to be inert gases. In any case, it should be emphasized that the results shown in Fig. 5-7 can be interpreted by the proposed mixed-potential-mechanism.

Finally, we describe the dependence of the sensitivities to NO and NO<sub>2</sub> on the temperature. Our preliminary experiments revealed that the sensitivities to NO and NO<sub>2</sub> increased with decreasing temperature. This is likely due to more selective adsorption of NO or NO<sub>2</sub> than O<sub>2</sub> on the surface of the PtRh/C catalyst at lower tem-

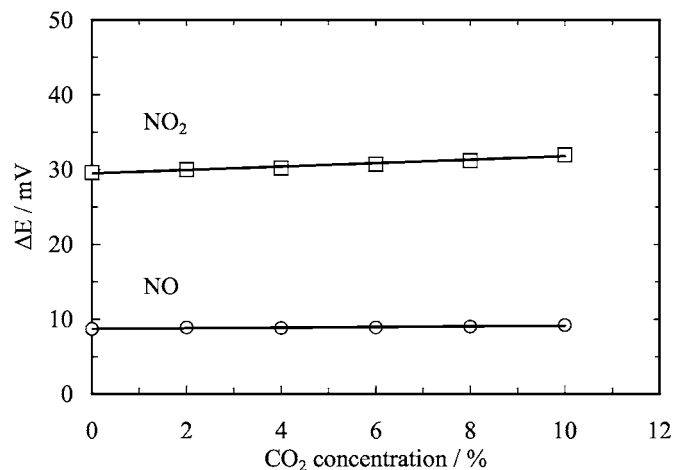


**Figure 7.** Dependences of sensitivities to 1000 ppm NO and 1000 ppm NO<sub>2</sub> on CO<sub>2</sub> concentration at 250°C. The water-vapor and O<sub>2</sub> concentration were maintained at constant values of 2.7 and 4%, respectively.

peratures. This not only supports the mixed-potential-mechanism proposed above, but also suggests that the sensitivities to NO and NO<sub>2</sub> would be further improved by the addition of a basic material such as alkaline earth carbonates to the PtRh/C, since NO<sub>x</sub> are acid molecules.<sup>27</sup>

### Conclusions

A sensor using a proton-conducting Sn<sub>0.9</sub>In<sub>0.1</sub>P<sub>2</sub>O<sub>7</sub> as the electrolyte exhibited largely positive emf values to both NO and NO<sub>2</sub>, which is a distinguishable characteristic from the results reported for the YSZ-based sensors. This was due to the mixed potential at the working electrode, wherein a cathodic reaction of NO or NO<sub>2</sub> and an anodic reaction of water vapor simultaneously proceeded. The dependences of the sensitivities to NO and NO<sub>2</sub> on the water-vapor and O<sub>2</sub> concentrations could be explained by using a mixed-potential-mechanism. The present sensor is shown to be a promising NO<sub>x</sub> sensor at intermediate temperatures. Additional experiments must be performed to establish the long-term reliability for actual applications.

*Nagoya University assisted in meeting the publication costs of this article.*

### References

1. N. Kato, K. Nakagaki, and N. Ina, SAE paper 960334 (1996).
2. N. Kato, Y. Hamada, and H. Kurachi, SAE paper 970858 (1997).
3. Y. Tan and T. C. Tan, *J. Electrochem. Soc.*, **141**, 461 (1994).
4. G. Lu, N. Miura, and N. Yamazoe, *Sens. Actuators B*, **35-36**, 130 (1996).
5. G. Lu, N. Miura, and N. Yamazoe, *J. Electrochem. Soc.*, **143**, L154 (1996).
6. H. Okamoto, H. Obayashi, and T. Kudo, *Solid State Ionics*, **1**, 319 (1980).
7. N. Miura, T. Raisen, G. Lu, and N. Yamazoe, *J. Electrochem. Soc.*, **144**, L198 (1997).
8. Y. Yan, N. Miura, and N. Yamazoe, *Chem. Lett.*, **1994**, 1733.
9. S. Thiemann, R. Hartung, U. Guth, and U. Schönauer, *Bioacoustics* **2**, 463 (1996).
10. T. Hibino, Y. Kuwahara, S. Wang, S. Kakimoto, and M. Sano, *Electrochem. Solid-State Lett.*, **1**, 197 (1998).
11. T. Hibino, A. Hashimoto, S. Kakimoto, and M. Sano, *J. Electrochem. Soc.*, **148**, H1 (2001).
12. R. Mukundan, E. L. Brosna, D. R. Brown, and F. H. Garzon, *Electrochem. Solid-State Lett.*, **2**, 412 (1999).
13. R. Mukundan, E. L. Brosna, D. R. Brown, and F. H. Garzon, *J. Electrochem. Soc.*, **147**, 1583 (2000).
14. F. H. Garzon, R. Mukundan, R. Lujan, and E. L. Brosna, *Solid State Ionics*, **175**, 487 (2004).
15. N. Miura, G. Lu, N. Yamazoe, H. Kurosawa, and M. Hasei, *J. Electrochem. Soc.*, **143**, L33 (1996).
16. N. Miura, G. Lu, and N. Yamazoe, *Solid State Ionics*, **136-137**, 533 (2000).
17. N. Miura, S. Zhuiykov, T. Ono, M. Hasei, and N. Yamazoe, *Sens. Actuators B*, **83**, 222 (2002).
18. T. Nakamura, Y. Sakamoto, K. Saji, and J. Sakata, *Sens. Actuators B*, **93**, 214 (2003).
19. N. F. Szabo and P. K. Dutta, *Solid State Ionics*, **171**, 183 (2004).
20. M. Nagao, A. Takeuchi, P. Heo, T. Hibino, M. Sano, and A. Tomita, *Electrochem. Solid-State Lett.*, **9**, A105 (2006).
21. P. Heo, H. Shibata, M. Nagao, T. Hibino, and M. Sano, *J. Electrochem. Soc.*, **153**, A897 (2006).
22. M. Nagao, T. Yoshii, T. Hibino, M. Sano, and A. Tomita, *Electrochem. Solid-State Lett.*, **9**, J1 (2006).
23. H. Ohtsuka, *Appl. Catal., B*, **33**, 325 (2001).
24. C. Yang, P. Costamagna, S. Srinivasan, J. Benziger, and A. B. Bocarsly, *J. Power Sources*, **103**, 1 (2001).
25. T. Nanba, C. Kohno, S. Masukawa, J. Uchisawa, N. Nakayama, and A. Obuchi, *Appl. Catal., B*, **46**, 353 (2003).
26. T. Hibino, A. Hashimoto, K. Mori, and M. Sano, *Electrochem. Solid-State Lett.*, **4**, H9 (2001).
27. M. Misono and T. Inui, *Catal. Today*, **51**, 369 (1999).